14th International Symposium on Turbulence and Shear Flow Phenomena (TSFP14)
Heidelberg, Germany, July 28–31, 2026

MULTI-SCALE ANALYSIS OF AMPLITUDE AND FREQUENCY MODULATION IN TURBULENT BOUNDARY LAYERS

Abhishek Tyagi
Department of Aerospace Engineering
Indian Institute of Science
Bengaluru, Karnataka 560012, India
tabhishek@iisc.ac.in

Sourabh S. Diwan
Department of Aerospace Engineering
Indian Institute of Science
Bengaluru, Karnataka 560012, India
sdiwan@iisc.ac.in

ABSTRACT

We investigate multiscale amplitude modulation (AM) and frequency modulation (FM) in turbulent boundary layers (TBLs) using single-point hot-wire data from the literature at $Re_\tau \approx 15{,}000$ (Baars et al., 2015, 2017) and $Re_\tau \approx 2{,}600$ (Diwan & Morrison, 2018). Following the multiscale framework of Liu et al. (2019), scales are grouped as small scales ($\lambda < 0.3\delta$), large-scale motions (LSMs, 0.3δ–3δ), and very-large-scale motions (VLSMs, $\lambda > 3\delta$). Two systematic cutoff sweeps are performed. In the first, the small-scale band is fixed while the large-scale cutoff is varied; the AM coefficient rises and reaches a broad maximum, showing that modulation is supported by a finite range of large scales rather than a narrowband of wavelengths. In the second, the large-scale band is fixed using the cutoff identified from the first exercise, while the small-scale cutoff is varied; AM increases monotonically as small scales get finer. We extend the multiscale analysis to the buffer layer, a dynamically important region of the TBL not covered in the ASL study of Liu et al. (2019). In both exercises, the same pattern of increased AM with greater scale separation is observed, with the buffer layer exhibiting the strongest modulation levels. We also find a directional asymmetry: VLSMs do not effectively modulate the LSM band, consistent with Liu et al. (2019). However, in contrast to their ASL findings, LSMs in the present TBL do modulate the smaller scales effectively—suggesting that the strength of modulation depends on the degree of scale separation rather than on which specific band acts as the modulator. We also carry out multiscale FM analysis using the wavelet-based method of Baars et al. (2015). FM shows the same overall directional trends as AM but with a less orderly response at both Reynolds numbers. These results demonstrate that modulation in TBLs is strongly scale-dependent and that the strongest interaction occurs between well-separated scales.

INTRODUCTION

Turbulent boundary layers (TBLs) contain a wide range of interacting scales, and this complexity increases with Reynolds number. High-Reynolds-number TBLs are important both fundamentally—because of their well-separated scales (Hutchins & Marusic, 2007)—and practically, due to engineering relevance. A key challenge is to determine how these scales interact, at a given location and over two different locations. To address this, metrics such as amplitude modulation (AM) and frequency modulation (FM) have been employed. Most AM studies at low to moderate Reynolds numbers divide scales into two groups, large and small, which obscures details of multiscale interactions. There are only a few studies that have examined modulation across multiple scale combinations. They either deal with very high-Reynolds-number TBLs or the atmospheric surface layer (ASL), where strong scale separation and energetic very-large-scale motions (VLSMs) make inner–outer interaction prominent (Mathis et al., 2009; Liu et al., 2019). At laboratory-scale Reynolds numbers, the natural scale separation is inherently weak compared to the ASL; nevertheless, a multiscale study in this regime can still reveal interesting features of the interaction between different scale bands.

Several approaches have been proposed to quantify AM in a TBL. Bandyopadhyay & Hussain (1984) introduced an envelope-extraction method based on taking the absolute value of the high-pass filtered signal, followed by low-pass filtering; this was used later by Guala et al. (2011). Mathis et al. (2009) employed the Hilbert transform to define the small-scale envelope, which has since become a standard practice. Baars et al. (2015) introduced a wavelet-based approach, using the instantaneous standard deviation of the small-scale signal as a surrogate for the Hilbert-derived envelope. FM has received comparatively less attention, with approaches such as binning small-scale peaks relative to large-scale fluctuations (Ganapathisubramani et al., 2012) and wavelet-based instantaneous frequency (Baars et al., 2015) being used for its quantification.

In this study, we extend the above frameworks to investigate multiscale AM and FM using experimental TBL data from the literature at two Reynolds numbers: $Re_\tau \approx 15{,}000$ from the Melbourne facility (Baars et al., 2015, 2017) and $Re_\tau \approx 2{,}600$ from Diwan & Morrison (2018). Our analysis follows the multiscale framework of Liu et al. (2019), originally applied to the log region of the ASL, but here we extend it to cover the buffer region through to the mid-logarithmic region. In the present paper, scales below 0.3δ are treated as small scales, scales between 0.3δ and 3δ as large-scale motions (LSMs), and scales above 3δ as very-large-scale motions (VLSMs), following the classification of Balakumar & Adrian (2007) also adopted by Liu et al. (2019). For comparison with Liu et al. (2019), we use the same cutoffs for both of our data sets. However, in the low-Reynolds-number TBL, the weaker scale separation means that the lower LSM cutoff at 0.3δ passes through the near-wall inner peak. We therefore also shift this cutoff to 1δ and 2δ to check whether the observed trends remain robust when this overlap is reduced.

DATA AND METHODOLOGY

Both data sets described in the Introduction consist of single-point hot-wire measurements of streamwise velocity at several wall-normal locations covering the entire boundary-

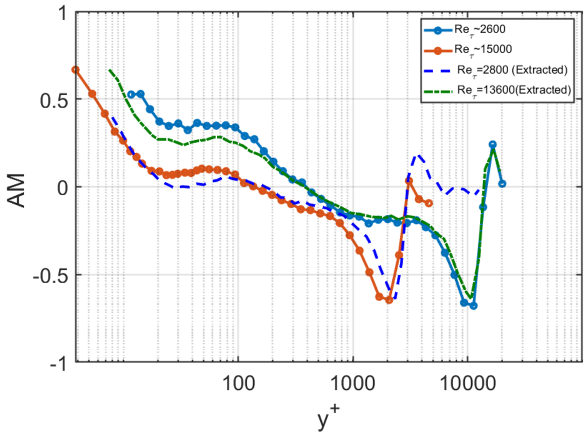

Figure 1. Validation of the numerical code. AM coefficient as a function of wall-normal distance with the nominal cutoff $\lambda/\delta = 1$. Present calculations compared with data extracted from Mathis et al. (2009).

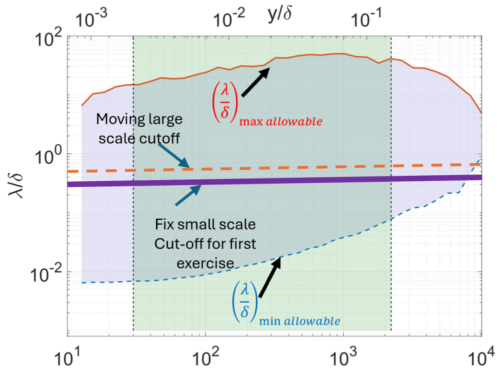

Figure 2. Cutoff-selection strategy. The 0.1-level contour of the normalized premultiplied energy spectrogram defines the energetic envelope. The lower envelope sets the minimum small-scale cutoff and the upper envelope sets the maximum large-scale cutoff, ensuring that all sweeps remain within energetically significant regions.

layer thickness. The three-band scale classification, as described in the Introduction, is used throughout.

The following are the definitions of AM and FM used in this study. Amplitude modulation is quantified as the normalized correlation between the large-scale velocity component and the large-scale part of the envelope of the small-scale signal (Mathis et al., 2009):

$$\mathrm{AM} = \frac{\langle u_L E_L(u_S)\rangle}{\langle u_L^2\rangle^{1/2}\langle E_L(u_S)^2\rangle^{1/2}}, \tag{1}$$

where u_L and u_S denote the large- and small-scale components of the streamwise velocity fluctuation, respectively, and $E_L(u_S)$ is the low-pass-filtered envelope of the small-scale signal obtained via the Hilbert transform.

Frequency modulation is evaluated using the wavelet-based instantaneous-frequency method of Baars et al. (2015):

$$\mathrm{FM} = \frac{\langle u_L f'_{S,L}\rangle}{\langle u_L^2\rangle^{1/2}\langle (f'_{S,L})^2\rangle^{1/2}}, \tag{2}$$

where $f'_{S,L}$ is the large-scale fluctuation of the instantaneous small-scale frequency. The instantaneous small-scale frequency $f_S(t)$ is obtained as the centroid of the local wavelet power spectrum over the small-scale range; the detailed procedure is described in Baars et al. (2015).

RESULTS AND DISCUSSION

Before proceeding further, we present a validation of our numerical code. Figure 1 shows the standard AM variation (for the cutoff $\lambda/\delta = 1$) with wall-normal distance, compared with data extracted from Mathis et al. (2009) at similar Reynolds numbers. Our results are consistent with the published data. Next, we present exercises to investigate multiscale interactions in the TBL.

Exercise 1: Fixed small scales, variable large-scale range

In the first exercise, the small scales are fixed to wavelengths shorter than λ_{HP}/δ ($\lambda_{HP} = 0.3\delta$), while the large-scale cutoff is swept from $\lambda_{LP} = 0.5\delta$ up to 30δ. Here, the subscripts HP and LP denote the high-pass and low-pass cutoffs, respectively. To ensure that only energetic scales are included, the premultiplied spectra are normalized by the global maximum of spectral energy, and the 0.1 contour level is extracted from the spectrogram (figure 2). This contour defines the energetic envelope, with the lower envelope giving the minimum λ_{HP}/δ and the upper envelope giving the maximum λ_{LP}/δ at each wall-normal location. As shown schematically in figure 2, the purple line marks the fixed small-scale bound $\lambda_{HP}/\delta = 0.3$ while the red dashed line indicates the large-scale cutoff λ_{LP} being swept upward. The energetic envelope constrains only these cutoff positions—the upper limit of the small-scale filter and the lower limit of the large-scale filter—so that the red dashed line never crosses the upper envelope; the filtered signals themselves include all scales below and above these limits, respectively.

This analysis is conducted from the buffer layer up to the mid-logarithmic region, where amplitude modulation (AM) typically changes sign from positive to negative when using the nominal cutoff of $\lambda = \delta$. In figure 3(a), increasing the large-scale lower cutoff from the lower to the upper limit causes AM to rise and reach a maximum, beyond which AM shows a gradual decrease. When the upper limit of the sweep is extended beyond 30δ, some AM curves at specific wall-normal locations show a more rapid decline; however, these ranges are also restricted by the minimum energetic envelope, and such results are not shown here. The broad maximum and plateau behaviour observed for most of the logarithmic region is consistent with the ASL results of Liu et al. (2019), who also report broad plateaus at comparable wall-normal locations. However, in their data a few wall-normal locations near the lower end of the log layer exhibit comparatively narrow peaks, a feature that is less prominent in the present TBL data.

When a similar exercise is repeated for the moderate-Reynolds-number case ($Re_\tau \approx 2{,}600$), the results are qualitatively similar but there is no clear maximum as in the high-Re_τ TBL; instead, the curves show a gradual and sustained increase without reaching saturation. The inset in figure 3(a) presents the corresponding data at comparable y^+ for $Re_\tau \approx 2{,}600$, and one can clearly see this difference.

Thus, for a fixed range of small scales, AM generally increases as the large-scale cutoff moves farther from this range,

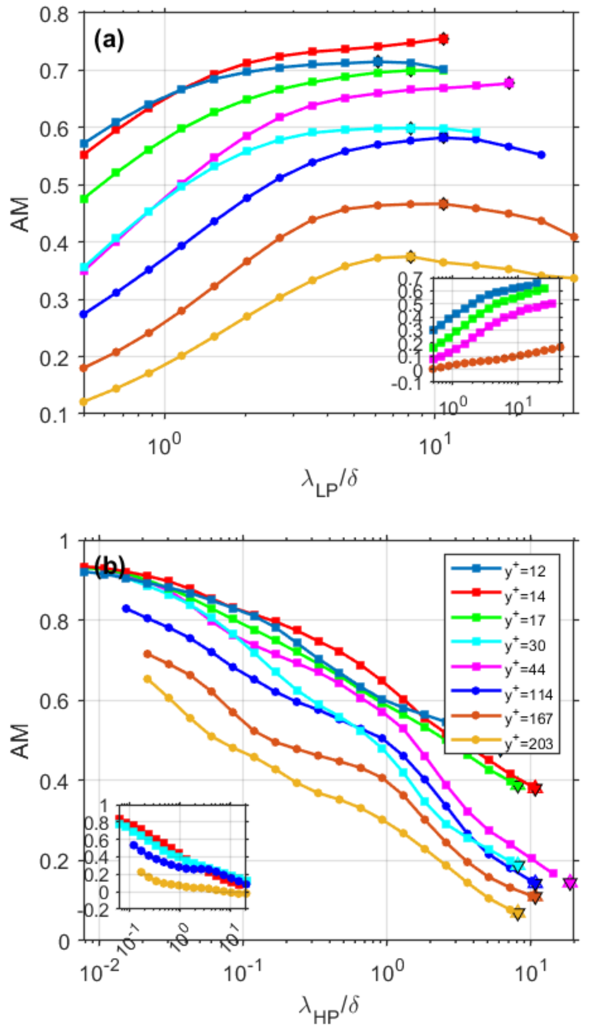

Figure 3. AM coefficient at $Re_\tau \approx 15{,}000$. (a) Exercise 1: fixed small scales ($\lambda/\delta < 0.3$), large-scale cutoff λ_{LP}/δ swept. Inset: same exercise for the $Re_\tau \approx 2{,}600$ TBL; colours represent the same y^+ locations as in the main panel. (b) Exercise 2: fixed large scales (cutoff from Exercise 1), small-scale cutoff λ_{HP}/δ swept. Inset: same exercise for the $Re_\tau \approx 2{,}600$ TBL; colours represent the same y^+ locations as in the main panel. Rectangular symbols: buffer-region locations; circular symbols: log-region locations.

before reaching a maximum (and in some cases decreasing at very low-energy large scales). This indicates that not all large scales are equally effective modulators. We therefore define the most effective large-scale cutoff as the point where AM attains its maximum value. These cutoffs are then used as the lower limits of the large-scale band at the respective wall-normal locations for the subsequent exercise.

Exercise 2: Fixed large scales, variable small-scale range

In the second exercise, the large-scale cutoff from Exercise 1 is kept fixed, and the small-scale cutoff is swept downward from just below this cutoff to the lower limit of the energetic envelope (figure 2). As shown in figure 3(b), AM increases monotonically as the small-scale cutoff moves toward finer scales. Unlike in the ASL study by Liu et al. (2019), no plateau or local maximum is observed even within the log layer; instead, AM attains its highest values at the smallest energetically admissible scales. In the buffer region, AM values reach 0.85–0.90 (at certain wall-normal locations), which is remarkably high. This suggests that the most effective large-scale modulators act most strongly on the smallest available scales, highlighting that modulation becomes more efficient as the scale separation between large and small motions increases. The overall trend for the $Re_\tau \approx 2{,}600$ case is the same (see inset in figure 3b); the magnitude is simply shifted downward compared to the $Re_\tau \approx 15{,}000$ case.

Modulation of small scales by LSMs

In addition to the above exercises, we evaluate the capacity of LSMs to be modulated by VLSMs and to modulate the small scales. Liu et al. (2019) reported that LSMs are not effective in either role. In our study, we likewise find that LSMs are not effectively modulated by VLSMs (figure 4a). However, they do exhibit a noticeable capacity to modulate the small scales (figure 4b), although their influence is weaker compared to that of VLSMs. Moreover, as shown in figure 4(b), lowering the cutoff that separates LSMs from the small scales leads to progressively stronger AM. One thing to note is that LSMs and VLSMs are structures found in the log layer (Balakumar & Adrian, 2007), and in the buffer layer what we measure is effectively their footprints. The nomenclature used here does not cause any issue because the lower limit of the LSM band (0.3δ) still lies above the near-wall spectral peak, which represents the near-wall small scales or streaks. In the case of the LSM-to-small-scale interaction, as we move closer to the wall and into the buffer region (which was not covered in the ASL study of Liu et al. 2019), LSMs show a clear ability to modulate the small scales, since the near-wall region is more populated by finer-scale motions. Here too, band separation is the key factor: what matters for AM is not whether the large scales are classified as LSMs or VLSMs, but how far separated they are from the small scales.

For the $Re_\tau \approx 2{,}600$ case, the overall behavior remains similar (figure 7c,d). The VLSM$\rightarrow$LSM interaction is still weak, with only a small positive AM at some near-wall locations and no clear wall-normal behaviour. In contrast, the LSM$\rightarrow$small-scale interaction shows the same dependence on scale separation as in the $Re_\tau \approx 15{,}000$ case, but at a consistently lower level, indicating a Reynolds-number-dependent reduction in amplitude. At this lower Reynolds number, however, the nominal lower LSM cutoff of 0.3δ passes through the near-wall inner spectral peak, so the fixed cutoff does not cleanly separate small and large scales close to the wall. To assess whether these observations are a consequence of poor scale separation in the near-wall buffer region, we also carry out band-sensitivity tests, discussed later.

FREQUENCY MODULATION

The same two exercises described above for AM are repeated for the FM analysis (figure 5). The overall directional trends are similar: FM increases as more large scales are included in the modulating signal, and it also increases as the small-scale cutoff is moved toward finer scales. However, the FM response is noticeably less orderly than the corresponding AM at both Reynolds numbers.

In Exercise 1, at $Re_\tau \approx 15{,}000$ (figure 5a), the FM curves are either saturated or only weakly increasing, and they also intersect each other at several points. This implies that the increment of FM with the same range of large scales is not as grad-

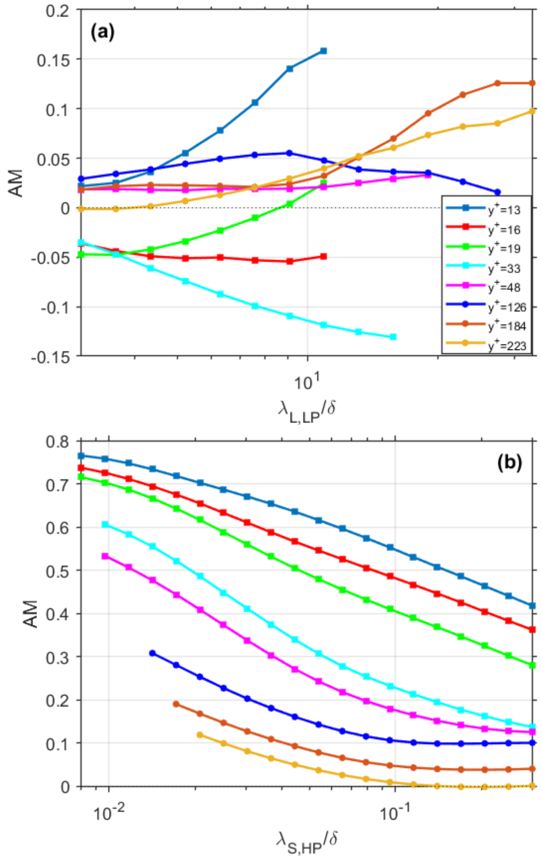

Figure 4. LSM-related AM at $Re_\tau \approx 15{,}000$. (a) VLSM→LSM: AM of the LSM band ($0.3 \leq \lambda/\delta \leq 3$) modulated by VLSMs ($\lambda/\delta > 3$). (b) LSM→small scales: AM of small scales ($\lambda/\delta < 0.3$) modulated by the fixed LSM band. Symbols as in figure 3.

ual as in the AM case, and hence the range of effective large scales that modulate the smaller ones may not be the same as for AM. At $Re_\tau \approx 2{,}600$ (inset in figure 5a), the buildup is more gradual and no clear saturation is reached within the plotted range.

In Exercise 2, the trend is more or less recovered: FM increases as the small-scale cutoff is moved toward finer scales. However, the FM curves remain less orderly than their AM counterparts at both Reynolds numbers. At $Re_\tau \approx 15{,}000$ (figure 5b) the trends are broadly monotonic but show flattening, crossings between wall-normal locations, and patches of weak non-monotonicity that are absent in the corresponding AM. At $Re_\tau \approx 2{,}600$ (inset in figure 5b) the irregularity is more pronounced: some curves level off, some recover at the largest λ_{HP}/δ, and some outer locations approach zero or turn weakly negative over part of the sweep.

FM of the LSM interactions

The same directional asymmetry observed in AM also appears in FM (figure 6). When the LSM band is treated as the modulated band and the VLSM cutoff is swept, the FM remains weak at both Reynolds numbers (figure 6a). The values stay small, are sensitive to sign, and do not show any clear wall-normal trend. The VLSM-to-LSM frequency modulation is therefore weak, just like the corresponding AM.

For the LSM-to-small-scale interaction (figure 6b), the FM becomes clearly positive and increases as the small-scale cutoff decreases. At $Re_\tau \approx 15{,}000$, this interaction is strong and well organized, with the largest values in the buffer layer. At $Re_\tau \approx 2{,}600$, the FM is weaker but follows the same trend (results not shown here).

BAND-SENSITIVITY TESTS

The scale cutoffs used in this study were chosen for comparison with the ASL results of Liu et al. (2019). Since we extend our analysis to the buffer layer, some additional clarity is needed regarding the applicability of these cutoffs in the near-wall region. LSMs and VLSMs are structures found in the log layer, and their cutoffs are used as a rule of thumb following Balakumar & Adrian (2007). In the buffer region, the near-wall spectral peak is the signature of small scales (streaks), and LSMs and VLSMs only show their presence there in the form of footprints.

For the $Re_\tau \approx 15{,}000$ case, the premultiplied spectrogram (figure 7a) shows that the 0.3δ separation lies above the near-wall spectral peak, so the small-scale and large-scale definitions are not affected. However, for the $Re_\tau \approx 2{,}600$ case, the premultiplied spectrogram (figure 7b) shows that the 0.3δ cutoff actually cuts through the near-wall spectral peak itself, and hence the fixed LSM band contains near-wall small scales too. To avoid this, we shift the lower limit of the LSM band to 1δ and then to 2δ, which places it above the inner spectral peak (or at least avoids cutting through it). Both the AM and FM metrics are then recomputed.

VLSM→LSM interaction. In both AM and FM, the small correlation obtained with the nominal 0.3–3δ band at $Re_\tau \approx 2{,}600$ collapses toward zero when the lower edge is raised to 1δ and 2δ (figure 7c). Doing so actually decreases the band separation with the VLSM range, and the already weak modulation in the 0.3δ case becomes much weaker. Combined with the already weak response observed at $Re_\tau \approx 15{,}000$, this confirms that the VLSM-to-LSM interaction is intrinsically weak at both Reynolds numbers.

LSM→small-scale interaction. When the lower edge is raised from 0.3δ to 1δ and then to 2δ, the modulation becomes stronger at $Re_\tau \approx 2{,}600$ (figure 7d). This is because the spectrally mixed lower portion of the LSM band was diluting the modulation signature rather than contributing to it. Once excluded, the remaining upper part of the LSM range ($\lambda/\delta \gtrsim 1$) produces a clearer and stronger modulation of the finer scales, which is again consistent with increased scale separation between the LSM band and the small scales.

The band-sensitivity tests confirm that the weak VLSM-on-LSM modulation is a robust result, not a band-definition artifact.

CONCLUSIONS

A multiscale analysis of amplitude modulation (AM) and frequency modulation (FM) has been carried out in turbulent boundary layers at $Re_\tau \approx 15{,}000$ and $Re_\tau \approx 2{,}600$, by using the framework of Liu et al. (2019) for the logarithmic and buffer regions. The main findings are as follows.

1. For a fixed small-scale band, AM increases as the large-scale cutoff is moved to larger wavelengths and reaches a broad maximum, indicating that modulation is supported by a finite range of large scales. At low Reynolds number, no clear maximum is observed; instead the curves show a gradual and sustained increase.
2. For a fixed large-scale band, AM increases monotonically as the small-scale cutoff is pushed toward finer scales,

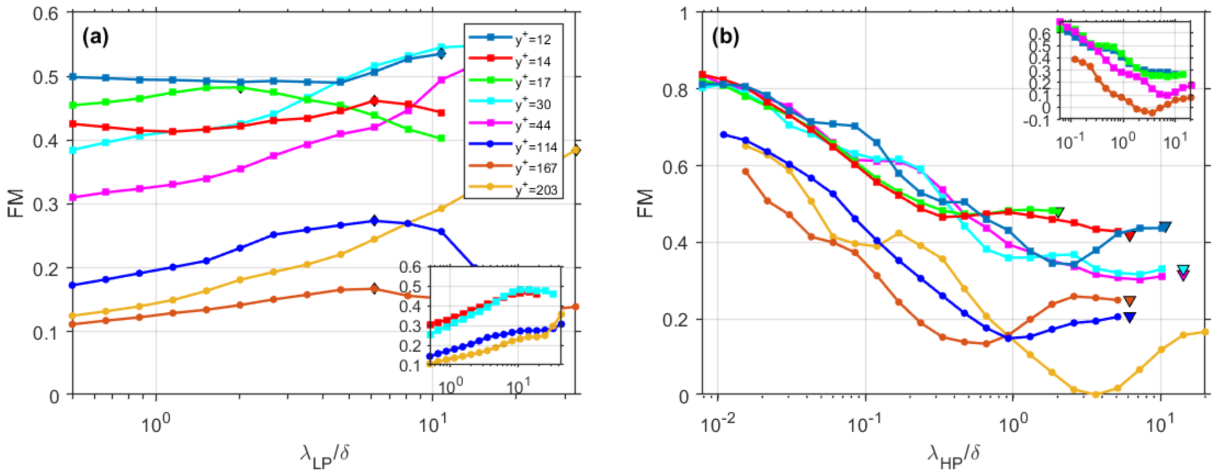

Figure 5. Frequency modulation from the large-scale and small-scale cutoff sweeps. (a) Large-scale sweep at $Re_\tau \approx$ 15,000 for fixed small scales ($\lambda/\delta < 0.3$); inset shows $Re_\tau \approx$ 2,600. (b) Small-scale sweep at $Re_\tau \approx$ 15,000 for fixed large scales; inset shows $Re_\tau \approx$ 2,600. Rectangular symbols: buffer-region locations; circular symbols: log-region locations.

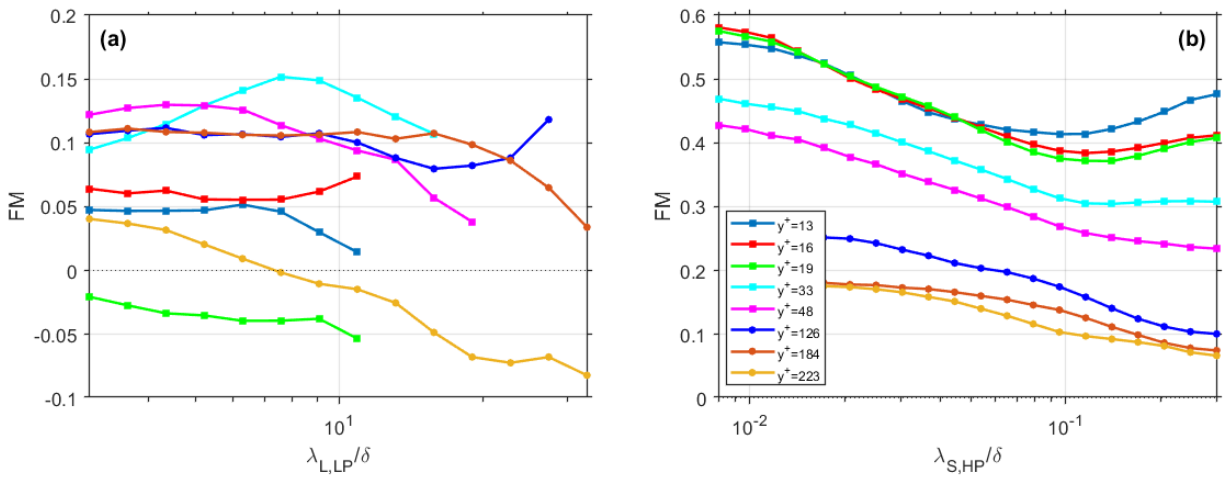

Figure 6. FM of the LSM-related interactions. (a) VLSM→LSM: FM of the LSM band ($0.3 \leq \lambda/\delta \leq 3$) with the VLSM cutoff swept. (b) LSM→small scales: FM of small scales ($\lambda/\delta < 0.3$) modulated by the fixed LSM band. Symbols as in figure 5.

with buffer-layer values reaching 0.85–0.90. This confirms that modulation is strongest when the interacting scales are well separated.

3. VLSMs do not effectively modulate the LSM band, consistent with Liu et al. (2019). However, unlike their ASL findings, LSMs in the present TBL do modulate the smaller scales effectively. This shows that the degree of scale separation, rather than the nominal classification of the modulating band, controls the strength of modulation. This finding is likely related to two factors: first, our analysis extends to the buffer layer where the small scales are finer and hence even LSMs have sufficient scale separation to produce meaningful modulation—a region not covered by Liu et al. (2019); and second, at laboratory Reynolds numbers the relative energy content of LSMs compared to VLSMs is higher than in the ASL. Separating these two effects requires further investigation.
4. The FM analysis, presented here for the first time, shows the same directional trends as AM but with a less orderly response. In Exercise 1, the FM curves show saturation and mutual crossings, suggesting that the range of effective modulating scales may differ from that for AM. In Exercise 2, the monotonic trend with finer small scales is recovered.
5. Band-sensitivity tests confirm that the VLSM-to-LSM interaction is intrinsically weak at both Reynolds numbers. Raising the lower LSM boundary from 0.3δ to 1δ and 2δ strengthens the LSM-to-small-scale modulation, consistent with increased scale separation once the spectrally mixed content near the inner peak is excluded.

An interesting trend emerges when comparing the ASL data of Liu et al. (2019) with our two Reynolds numbers: in Exercise 1, the AM curves show clear peaks or plateaus in the ASL, broader plateaus at $Re_\tau \approx$ 15,000, and no clear maximum at $Re_\tau \approx$ 2,600—the curves simply keep rising. That is, the tendency to reach saturation reduces as Reynolds number decreases. This can be understood from the spectral structure. At high Reynolds number, the energy spectrum has distinct, well-separated peaks (inner, LSM, VLSM) with clear gaps between them. Once the dominant modulating peak is captured in the sweep, adding more scales contributes little, and the curve saturates. At lower Reynolds number, these

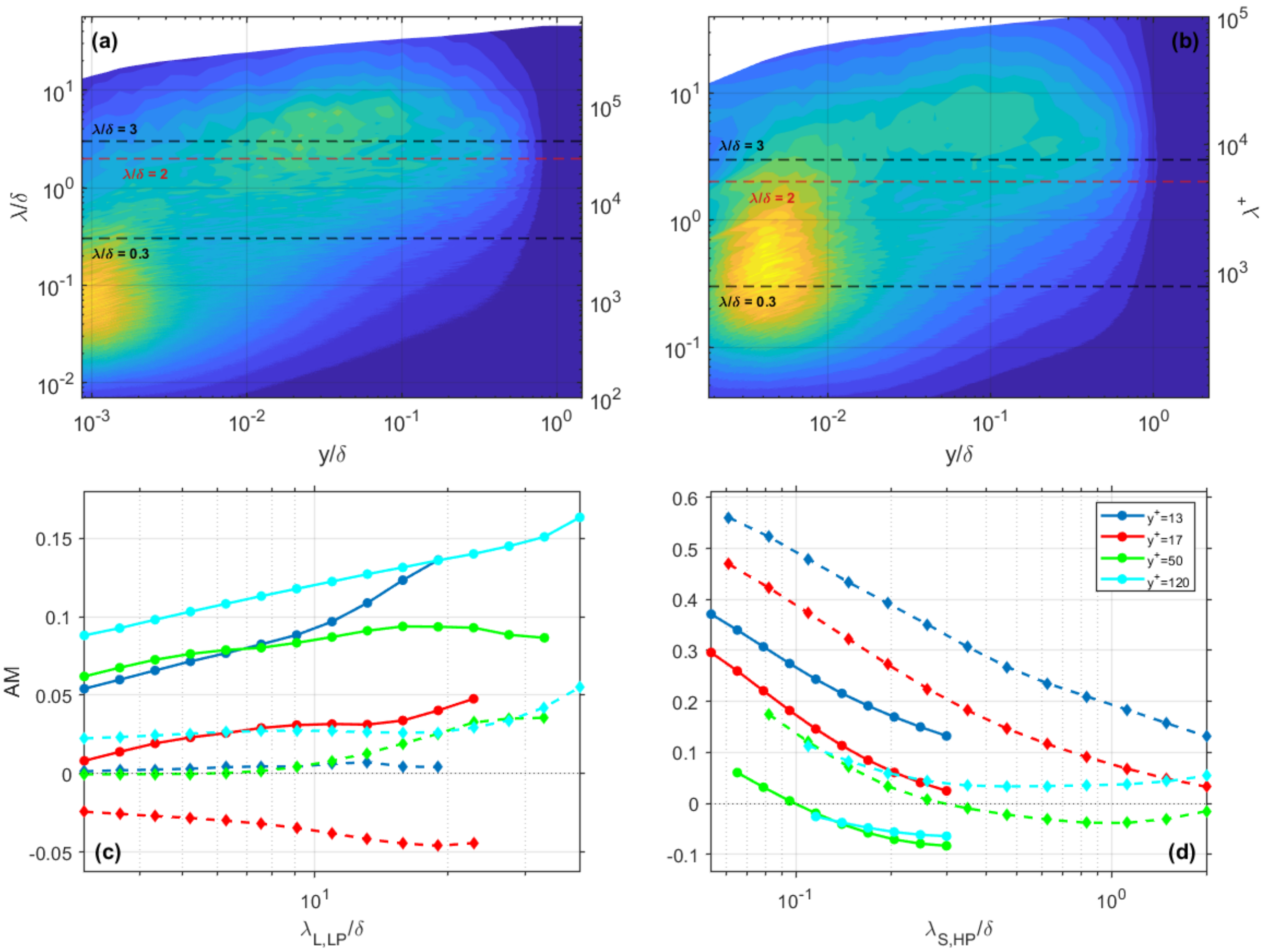

Figure 7. Band-sensitivity tests at $Re_\tau \approx 2{,}600$. (a) Premultiplied spectrogram at $Re_\tau \approx 15{,}000$. (b) Premultiplied spectrogram at $Re_\tau \approx 2{,}600$. (c) VLSM→LSM: AM with the nominal 0.3–3δ band and the narrower 2–3δ band for selected y^+ locations. (d) LSM→small scales: AM with the nominal 0.3–3δ band and narrower LSM bands for selected y^+ locations. In (c) and (d), solid lines with circles denote the 0.3–3δ band and dashed lines with diamonds denote the narrower bands.

gaps shrink and the energy is spread more continuously across scales. There is no single dominant modulating band causing saturation, so each additional large scale still adds to the modulation. Scale separation thus becomes the controlling factor.

ACKNOWLEDGEMENT

We thank Prof. Ivan Marusic, University of Melbourne, for making the TBL data at $Re_\tau \approx 15{,}000$ available.

REFERENCES

Baars, W. J., Talluru, K. M., Hutchins, N., and Marusic, I., 2015, "Wavelet Analysis of Wall Turbulence to Study Large-Scale Modulation of Small Scales," *Exp. Fluids*, Vol. 56, Article 188.

Baars, W. J., Hutchins, N., and Marusic, I., 2017, "Reynolds-Number Trend of Hierarchies and Scale Interactions in Turbulent Boundary Layers," *Phil. Trans. R. Soc. A*, Vol. 375, Article 20160077.

Balakumar, B. J., and Adrian, R. J., 2007, "Large- and Very-Large-Scale Motions in Channel and Boundary-Layer Flows," *Phil. Trans. R. Soc. A*, Vol. 365, pp. 665–681.

Bandyopadhyay, P. R., and Hussain, A. K. M. F., 1984, "The Coupling Between Scales in Shear Flows," *Phys. Fluids*, Vol. 27, pp. 2221–2228.

Diwan, S. S., and Morrison, J. F., 2018, "Spectral Structure and Linear Mechanisms in a Rapidly Distorted Boundary Layer," *Int. J. Heat Fluid Flow*, Vol. 72, pp. 61–78.

Ganapathisubramani, B., Hutchins, N., Monty, J. P., Chung, D., and Marusic, I., 2012, "Amplitude and Frequency Modulation in Wall Turbulence," *J. Fluid Mech.*, Vol. 712, pp. 61–91.

Guala, M., Metzger, M., and McKeon, B. J., 2011, "Interactions within the Turbulent Boundary Layer at High Reynolds Number," *J. Fluid Mech.*, Vol. 666, pp. 573–604.

Hutchins, N., and Marusic, I., 2007, "Evidence of Very Long Meandering Features in the Logarithmic Region of Turbulent Boundary Layers," *J. Fluid Mech.*, Vol. 579, pp. 1–28.

Liu, H., Wang, G., and Zheng, X., 2019, "Amplitude Modulation Between Multi-Scale Turbulent Motions in High-Reynolds-Number Atmospheric Surface Layers," *J. Fluid Mech.*, Vol. 861, pp. 585–607.

Mathis, R., Hutchins, N., and Marusic, I., 2009, "Large-Scale Amplitude Modulation of the Small-Scale Structures in Turbulent Boundary Layers," *J. Fluid Mech.*, Vol. 628, pp. 311–337.